# Polymers imprinted with three REG1B peptides for electrochemical determination of Regenerating Protein 1B, a urinary biomarker for pancreatic ductal adenocarcinoma

**Jurcevic, S., Lee, M-H., Thomas, J.L., Liao, C-L., Crnogorac-Jurcevic, T. and Lin, H-Y.**

This is an author's accepted manuscript of an article published in Microchimica Acta, 184 (6), p. 1773–1780, 2017.

The final publication is available at Springer via:

https://dx.doi.org/10.1007/s00604-017-2169-4

# Rational epitope imprinting of REG1B peptides for electrochemical determination of pancreatic cancer in urine

*Mei-Hwa Lee[1], James L. Thomas[2], Chun-Lin Liao[1], Stipo Jurcevic[3], Tatjana Crnogorac-Jurcevic[4] and Hung-Yin Lin[5,*]*

***[1]Department of Materials Science and Engineering, I-Shou University, Kaohsiung 840, Taiwan***

***[2]Department of Physics and Astronomy, University of New Mexico, Albuquerque, NM 87131, USA***

***[3]Department of Biomedical Sciences, University of Westminster, London W1W 6UW, United Kingdom***

***[4]Barts Cancer Institute, Queen Mary University of London, London EC1M 6BQ, United Kingdom***

***[5]Department of Chemical and Materials Engineering, National University of Kaohsiung, Kaohsiung 81148, Taiwan***

* To whom correspondence should be addressed:
Department of Chemical and Materials Engineering,
National University of Kaohsiung (NUK),
700, Kaohsiung University Rd.,
Nan-Tzu District, Kaohsiung 811, Taiwan
Tel: (O) +886(7)591-9455; (M) +886(912)178-751
E-Mail: linhy@ntu.edu.tw or linhy@caa.columbia.edu

**Abstract**

Three peptides (each containing 13 - 18 amino acids) were synthesized and used as templates for molecular imprinting and epitope recognition of the regenerating Protein 1B (REG1B), which is one of the urinary biomarkers for pancreatic ductal adenocarcinoma (PDAC). Poly(ethylene-co-vinyl alcohol)s were employed as the host for molecular imprinting of the peptides. Following their preparation, the molecularly imprinted polymers (MIP) were examined by cyclic voltammetry. The electrochemical responses of a screen-printed gold substrate coated with the MIP were measured at a working voltage of 300 mV (vs. Ag/AgCl); the entire protein and the peptides gave similar responses at concentrations of <1.0 pg·mL$^{-1}$, with detection limits as low as 0.1 pg·mL$^{-1}$. Urine samples from healthy and PDAC patients were then analyzed by using this modified gold electrode, and the results are in agreement with data obtained with ELISA.

Keywords: MIP; AFM; ESCA; Cyclic voltammetry; Hexacyanoferrate; Peptide imprinted polymer; pancreatic ductal adenocarcinoma (PDAC); Regenerating protein 1B (REG1B).

## Introduction

Molecularly imprinted polymers (MIPs) have been developed as a robust and inexpensive replacement for antibodies in the recognition of target molecules (e.g. antigens). Proteins like albumin, lysozyme, haemoglobin and myoglobin have been employed as model systems for the testing of protein imprinting [1]. Typically, the whole proteins have been used for molecular imprinting, although a few studies have tried to compare whole protein to peptide imprinting [2]. However, no general protocol has as yet been developed for the recognition of protein epitopes.

The approach of peptide, or epitope imprinting using a four amino acid peptide (YPLG, 4-mer) as the template to form a MIP (containing MAA and EGDMA) and then used for the recognition of a longer peptide (oxytocin) [3]. That group later compared MIPs using templates with amino acid substitutions (relative to the parent peptide hormone angiotensin II, 8-mer) [4]. A 15-mer peptide incorporating amino acids 90-95 of the Japanese encephalitis virus nonstructural protein 1 (NS1) Thr-Glu-Leu-Arg-Tyr-Ser-Trp-Lys-Thr-Trp-Gly-Lys -Ala-Lys-Met was chosen as the template for the recognition of Dengue virus protein by a quartz crystal microbalance (QCM) chip [5]. Imprinting porous silica scaffolds with a 16-residue peptide (from lysozyme C, 1.8 kDa) led to preferential binding of the whole protein (lysozyme, 14 kDa), compared to irrelevant protein targets. Tai's group has also

imprinted different combinations of tetrapeptides [6]; segments (9-mer to 14-mer) of Anthrax protective antigen ($PA_{83}$, 83 kDa) [7]; and nine different linear epitope sequences (11 – 15 mer), selected to prepare MIPs to recognize creatine kinase (CK) isozymes [8]. The rational selection of peptide epitope templates (8- to 10-mer) for the recognition of proteins (e.g. trypsin, thermolysin, pepsin, chymotrypsin and Arg-protenase) by MIPs was also discussed by Bossi *et al*. [9] Li's group intensively studied the sensing [10,11] and adsorption [12] of albumin by imprinting with 9- to 15-mer fragments [11] or with one or two mutated residues [10,12,11]. Multiepitope imprinting was also employed for the capture of proteins [13].

Electrochemical sensing is inexpensive, flexible and has demonstrable utility in point-of-care devices. Molecularly imprinted polymers (MIPs) hold out the possibility of adding selectivity and specificity, at low cost and without the stability and storage problems associated with biologically-derived molecular recognition. Piletsky and Turner [14], Blanco-López *et al.* [15], McCluskey *et al.* [16], Rao and Kala [17] and Suryanarayanan *et al.* [18] have reviewed electrochemical sensors using molecularly imprinted polymers as sensing elements. Small molecules (e.g. quercetin [19], theophylline [20], 3-hydroxyanthranilic [21] and imidacloprid [22]), proteins (e.g. albumin, lysozyme [23] and nuclear matrix protein 22 (NMP22) [24]) and even microorganisms (e.g. viruses [25], bacteria [26] and algae [27]) have been used as the imprinting templates. Moreover, molecularly imprinted polymers can be

integrated on microfluidic systems for either dielectric or electrochemical sensing of viruses [28] and urinary melatonin [29], respectively. The combination of MIPs and electrochemical analysis can thus be useful in a homecare system.

In this study, three peptides (13- to 18-mers) of Regenerating Protein 1B (REG1B) were selected for their solubility, and distinctiveness between homologous proteins REG1A, REG3, REG4 and Aggrecan. The peptides were synthesized and used as templates for the preparation of molecular imprinting and epitope recognition. Four poly(ethylene-*co*-vinyl alcohol)s containing ethylene mole % from 27 to 44 were employed to prepare the molecularly imprinted polymers by phase inversion, and the imprinted polymer electrodes were examined by electrochemical analysis. Finally, urine samples from healthy and pancreatic ductal adenocarcinoma (PDAC) patients were examined by peptide-imprinted EVAL-based sensors and the REG1B concentrations measured.

## Experimental Section

### Reagents and chemicals

Peptides (SCSGFKKWKDESCEKK (Peptide 2), KSWDTGSPSSANAGYCAS (Peptide 4), KESSTDDSNVWIG (Peptide 6) of REG1B were ordered from Yao-Hong Biotechnology Inc. (HPLC grade, New Taipei City, Taiwan; http://www.yh-bio.com.tw/). Urea, creatinine

(TLC ≧98%), albumin (from bovine serum, minimum 98%), sodium dodecyl sulphate (SDS) and poly(ethylene-*co*-vinyl alcohol) (abbreviated as EVAL) with ethylene 27, 32, 38 and 44 molar % were from Sigma-Aldrich Co. (St. Louis, MO; https://www.sigmaaldrich.com/). Dimethyl sulfoxide (DMSO) was purchased from Panreac (Barcelona, Spain; http://www.panreac.es/). Potassium ferrocyanide and potassium ferricyanide were both from J.T. Baker Chemical Co. (Center Valley, PA; http://jtbaker.com/). Potassium chloride was from Showa Chemical Industry Co., Ltd. (Tokyo, Japan; http://showa-chemical.co.jp/). De-ionized (DI) water, produced by a PURELAB Ultra (ELGA, Albania; http://www.elgalabwater.com/), used in the preparation of buffers and for rinse solutions was 18.2 MΩ·cm in resistivity. Human REG1B cloned in Escherichia coli (*E. coli*) (#g1004044D06) was purchased from Bioresource Collection and Research Center (BCRC; http://www.bcrc.firdi.org.tw/), Hsinchu, Taiwan. The culture medium for Escherichia coli contained Miller (Luria-Bertani) LB Broth (BD Difco™; http://www.bd.com/) and Ampicillin 100 μg/mL. All chemicals were used as received unless otherwise mentioned.

**The preparation of peptide-imprinted polymers coated sensing chips**

EVALs were dissolved in DMSO at the concentration of 0.1 wt% and with or without 1.0 $mg \cdot mL^{-1}$ of template peptides. EVAL will crystallize from DMSO as the solvent is

removed, as shown in the ternary water–DMSO–EVAL phase diagram [30], so polymer films are readily produced by evaporation of DMSO. The preparation of peptide-imprinted (MIPs) and non-imprinted (NIPs) EVAL thin films on the working electrodes consisted: (1) dropwise addition of 2 μL of the EVAL solution with or without 1.0 mg·mL$^{-1}$ of template peptides on a screen-printed gold substrate (4 mm diameter, DropSens, Spain; http://www.dropsens.com/); (2) place polymer-coated electrodes in an oven at 50 $^{o}$C for 6 h to enhance the evaporation of solvent; and then (3) removal of template peptides by washing with 10 mL of 0.1 wt % aqueous SDS and DI water three times.

**Electrochemical examination of peptides and REG1B with peptide-imprinted polymer-coated sensors**

The electrochemical analysis was performed by sample injection into a flow-cell (DRP-FLWCL, DropSens, Spain; http://www.dropsens.com/) for screen-printed electrodes. The working, counter and Ag/AgCl reference electrodes were covered by injecting ca.10 μL of an aqueous solution of 500 mM KCl, 20 mM $K_4Fe(CN)_6$ and 20 mM $K_3Fe(CN)_6$; the electrode in the flow-cell [29] was pre-wetted to ensure that the electrode surface is properly wet with the redox couple for the electrochemical response. The same volume of sample was then injected for measurements. The electrochemical reactions were controlled and monitored

with a potentiostat (608-1A, CH Instruments, Inc., Austin, TX; http://www.chinstruments.com/). The current response of the imprinted polymeric sensing electrodes was assessed using cyclic voltammetry. The potential was scanned from -0.6 V to 0.6 V at 0.1 $V \cdot s^{-1}$ and the effects of imprinted peptides, interferent molecules and real samples on the peak currents for the ferri-/ ferrocyanide system were recorded. Urine samples were collected from the PDAC patients and healthy volunteers. The study was approved by the Brent Medical Ethics Committee under REC reference no. 05/Q0408/65. Twenty microliters of urine samples were diluted to 20 mL with the previously mentioned ferri-/ ferrocyanide solution. An enzyme-linked immuno-sorbent assay (ELISA) kit SEK11638 (Sino Biological Inc.; http://tw.sinobiological.com/) was employed to examine the REG1B concentration in random urine samples. All measurements in this work were carried out with at least two replicates; data are expressed as means and standard deviations.

**Surface characterization of peptide-imprinted EVAL thin films**

Peptide- and non-imprinted EVAL films were freeze-dried before examination by a SEM (Hitachi S4800, Hitachi High-Technologies Co., Tokyo, Japan; http://www.hitachi-hightech.com/), by electron spectroscopy for chemical analysis (ESCA, Axis Ultra DLD, Kratos Analytical Inc., Manchester, UK; http://www.kratos.com/) and by

atomic force microscopy (AFM, Solver P47H-PRO, NT-MDT Moscow, Russia; http://www.ntmdt-si.com/). The cantilever for AFM was a "Golden" silicon probe (NSG01, NT-MDT) with 6 nm probe tip size and 144 kHz resonant frequency.

**Results and Discussion**

The amino acid sequences of the REG1B peptides for the epitope recognition are listed in Table 1. The "rational" 1st choice is peptide 2 in Fig. 1, the C-terminal 16 amino acids of the protein. Important non-homologous amino-acids between REG1A and REG1B are at position 147, Q (glutamine, polar) to K (lysine, positive charge); positions 152-53, VP (hydrophobic valine and aromatic proline) to ES (glutamic acid, negative charge and serine, polar); and position 156, D (aspartic acid, negative charge) to K (lysine, positive charge). This sequence has six charged amino acids (KKDEDK), which suggests it is exposed on the protein surface. Its solubility in polar solvents should be very good due to six charged amino acids and five polar (SSTQC) amino acids. In addition, there are two bulky, aromatic amino acids (FW) within the sequence. The difference between REG1A and REG1B compared to REG3, REG4 and Aggrecan is relatively modest but should be sufficient to prevent cross-reaction. Most of the peptide forms an extended loop with only a short stretch (positions 149-152) forming a beta-strand. Furthermore, negatively charged amino acids in positions

151/129 (secreted protein/crystal structure positions), 155/133 and 156/134 (DED) have been proposed to form a contiguous parallel stretch on the protein surface [31]. Interestingly, positions 150/128 and 157/135 (KK) were also proposed to contribute to the exposed charged residues on the protein surface. The choice of peptides 4 and 6 are explained in the Electronic Supporting Material.

Cyclic voltammetry was employed to prescreen for the optimal composition of the EVALs. The potential at peak current was found to be 300 mV, Fig. S2(a). Figs. S1(b)-(d) show the current density differences, using MIP-coated electrodes, arising from the presence of peptides 2, 4 and 6 at 1.0 $ng \cdot mL^{-1}$, for MIP coatings made from four different EVAL compositions. MIP electrodes formed from EVALs containing 27, 32 and 27 ethylene mole % had higher current density differences, compared to the other commercially available compositions, for peptides 2, 4 and 6, respectively. For example, the highest current density differences in the peptide 2 MIP- and NIP-coated electrodes were 75.85 ± 4.05 and 26.03 ± 5.71 $\mu A \cdot cm^{-2}$, respectively. Interestingly, the higher ethylene mole % of EVALs decreased the current density difference in both MIP- and NIP-coated electrodes. The imprinting effectiveness for the peptide-imprinted polymers is defined as the ratio of the current difference of MIPs and NIPs, measured with given concentrations of target molecules (*i.e.* peptides, in this study). The highest imprinting effectivenesses (IE) for peptide 4 was 2.6

(obtained by using EVAL containing 32 mole % of ethylene), and 2.9-3.0 for peptides 2 and 6 using 27 mole % ethylene of EVAL.

The effect of the concentration of peptides on optimized MIP and NIP-coated electrodes was further examined by using cyclic voltammetry. Figure 2(a) plots the cyclic voltammograms (CVs) of various peptide 2 concentrations on MIP electrodes; Figure 2(b) shows that the current density significantly increases with increasing concentration of peptide 2. Figures 2(c)-(d) show the response of MIP electrodes recognizing peptide 4 and peptide 6, compared to NIP electrodes of the same EVAL composition. In all cases, the MIP electrodes responded much more strongly than NIP electrodes, with imprinting effectiveness of 2-3. The ferrocyanide and ferricyanide ions are critical to the response in the cyclic voltammetry of electrochemical activity on MIP-coated electrodes [24]. MIP-coated electrodes have greater electrochemical activity in ferro/ferricyanide solution with more bound template or target (e.g. peptide/protein in this work), possibly due to some induced partial charge on the electrode surface [24].

The three optimized MIP sensors were then employed to measure the same *E coli* culture medium; the measured (or apparent) REG1B concentrations were 35.21±4.79, 82.60±4.04 and 45.03±2.62 $ng \cdot mL^{-1}$ by peptide 2-, 4- and 6-imprinted polymer-coated sensors, for sensors calibrated with peptides. The concentration measured by the peptide 4-imprinted

polymer-coated sensor is about 2-fold higher than that by peptide 2- and 6-imprinted polymer-coated sensors, which may due to the exposure peptides on the surface of REG1B. The actual concentration of REG1B was estimated at 78-213 ng/mL using an ELISA assay. Therefore, the peptide 4-imprinted polymer-coated electrodes were used for the latter real urine sample measurements.

The surface morphologies and nitrogen atomic concentrations of peptide 4 MIPs before and after template removal is shown in Fig. S3. When comparing the surface morphologies of peptide 4 MIPs before and after template removal in Figs. S3(a) and S3(b), the surface roughness seems higher for the surface before template removal. Moreover, nanoaggregates of size less than 50 nm can be found in Fig. S3(b). The nitrogen atomic profile in Fig. S2(c) showed the nitrogen surface concentration decreased from 2.83 to 0.33%, as expected when the nitrogen-rich template is removed by washing. A small amount of template molecules are likely still entrapped inside MIPs, but they may not reduce the recognition ability of MIPs. In Figs. S3(d) and (e), the surface roughness of the peptide 4 MIPs increased from 1.3 to 2.3 on removing target molecules and increased to 10.9 nm on target rebinding; however, the peptides may form nanoaggregates that are as large as 100 nm before binding on the MIP thin film. The aggregation of peptides may also reduce the electrochemical interactions between the surface of the MIP and target molecules, perhaps by affecting folding and unfolding. Note,

however, that aggregation can actually increase the responsive range of a MIP sensor by raising the upper limit for sensing to 1000 pg·mL$^{-1}$.

Finally, Table S1 summarizes analyses of six urine samples from the PDAC patients and healthy volunteers.. The REG1B in the samples fell in the range 0.47± 0.12 to 0.55±0.12 and 62.25± 7.01 to 205.48± 20.96 ng·mL$^{-1}$ for healthy volunteers and PDAC patients, respectively. These results are in agreement with measurements using enzyme-linked immunosorbent assay (ELISA) [32] in Table S1. The detectable range and sample volume with ELISA are about 3.13-200 pg·mL$^{-1}$ and 100 µL (www.sinobiologicalcdn.com/reagent/**SEK11638**.pdf), which is about 10 fold higher than the limit of detection of the MIP electrodes in this work. The urine samples from the healthy volunteers were not detectable because they were diluted 1000-fold for storage and transportation.

Additionally, the effects of interference by albumin, creatinine and urea in urine on the peptide 4 MIP electrodes are shown in Figure 3(a). The interference at 1.0 ng·mL$^{-1}$ did not give a current change higher than 23.45± 1.47 µA·cm$^{-2}$. Typically, the reference albumin concentration in random urine is less than 23 µg·mL-1 (i.e. 2.3 ng·mL$^{-1}$ after dilution ten thousand times for REG1B test). Fig. 3(b) depicts the comparison of the electrochemical signals of REG1B and peptide 4 titrated to the peptide 4 MIP sensor. Clearly, at lower concentration (less than 1.0 pg·mL$^{-1}$), the response of REG1B to peptide 4 MIP sensors is

very close to that of peptide 4, suggesting that the entire protein can participate in electron transfer processes. At higher concentrations, the response falls off slightly for the protein compared to the imprinted peptide. The electrochemical reaction results of peptide 4 and REG1B on peptide 4 imprinted EVAL (32 mol% ethylene) thin films were fit by the Hill equation, giving the maximum response for 154.93± 3.15 and 112.92± 2.97 $\mu A \cdot cm^{-2}$, respectively. The Hill equation, which can represent binding site cooperativity, has been used for the binding analysis of target molecules to MIP [33,34]: $\log(Y/(1-Y))=n \cdot \log[L]-n \cdot \log K_A$, where *Y* is the binding site occupancy, *n* the Hill coefficient, [F] the free ligand concentration and $K_A$ is the microscopic dissociation constant. The Hill coefficient (n) and microscopic dissociation constant ($K_A$) for the binding of peptide 4 and REG1B are 0.22, 10.95 $pg \cdot mL^{-1}$ and 0.17, 25.17 $pg \cdot mL^{-1}$, which give an equilibrium constant for dissociation ($K_d$) of around 1.69 - 1.73.

The MIP-based sensor remains stable for a long time and can be stored for reuse [35]; Figure S4 shows the reusability and reproducibility of measurements made with the peptide 4 MIP-coated electrode. The degradation in the electrochemical response of the electrode during the first five cycles was less than 10%, but may have been higher if the rebound target had not been completely removed. The reproducibility in the construction of MIP-based electrochemical sensors has been well established in other studies [21,36,24]. Long term

stability is also expected: EVAL MIP nanoparticles stored in darkness at room temperature for six months still show good sensitivity to target molecules [37]. The competitive recognition of the imprinted template and interferents is shown in Fig. 6. The relative current density differences were 95.01± 9.65, 87.64± 11.68, and 91.71±6.67 % when peptide 4 co-exists with albumin, creatinine or urea.

## Conclusions

Epitope recognition of proteins is important for both the binding of antibodies and for the preparation of the artificial antibodies (i.e. molecularly imprinted polymers). This study demonstrates the utility of rational selection of appropriate peptides as the templates for imprinting. The urine samples from patients with pancreatic cancer showed higher electrochemical response compared to samples from healthy controls, consistent with their expected elevated levels of the marker protein. The rational design of peptide-based molecularly imprinted polymers can be used for the epitope recognition of proteins, at far lower cost compared with whole protein imprinting. Thus, epitope imprinting shows great potential for future development of sensitive, diagnostic homecare sensors.

## Acknowledgements

We appreciate financial supports from Ministry of Science and Technology of ROC

under Contract nos. MOST 104-2220-E-390-001, MOST 104-2220-E-006-006, MOST 105-2918-I-214-001 and MOST105-2221-E-214-036-.

**References**

1. Ge Y, Turner APF (2008) Too large to fit? Recent developments in macromolecular imprinting. Trends in Biotechnology 26 (4):218-224

2. Turner NW, Jeans CW, Brain KR, Allender CJ, Hlady V, Britt DW (2006) From 3D to 2D: A Review of the Molecular Imprinting of Proteins. Biotechnology Progress 22 (6):1474-1489

3. Rachkov A, Minoura N (2000) Recognition of oxytocin and oxytocin-related peptides in aqueous media using a molecularly imprinted polymer synthesized by the epitope approach. Journal of Chromatography A 889 (1–2):111-118. doi:http://dx.doi.org/10.1016/S0021-9673(00)00568-9

4. Rachkov A, Hu M, Bulgarevich E, Matsumoto T, Minoura N (2004) Molecularly imprinted polymers prepared in aqueous solution selective for [Sar1,Ala8]angiotensin II. Analytica Chimica Acta 504 (1):191-197. doi:http://dx.doi.org/10.1016/S0003-2670(03)00764-5

5. Tai D-F, Lin C-Y, Wu T-Z, Chen L-K (2005) Recognition of Dengue Virus Protein Using Epitope-Mediated Molecularly Imprinted Film. Analytical Chemistry 77 (16):5140-5143. doi:10.1021/ac0504060

6. Tai D-F, Lin Y-F (2008) Molecularly imprinted cavities template the macrocyclization of tetrapeptides. Chemical Communications (43):5598-5600. doi:10.1039/B813439A

7. Tai D-F, Jhang M-H, Chen G-Y, Wang S-C, Lu K-H, Lee Y-D, Liu H-T (2010)

Epitope-Cavities Generated by Molecularly Imprinted Films Measure the Coincident Response to Anthrax Protective Antigen and Its Segments. Analytical Chemistry 82 (6):2290-2293. doi:10.1021/ac9024158

8. Tai D-F, Ho Y-F, Wu C-H, Lin T-C, Lu K-H, Lin K-S (2011) Artificial-epitope mapping for CK-MB assay. Analyst 136 (11):2230-2233. doi:10.1039/C0AN00919A

9. Bossi AM, Sharma PS, Montana L, Zoccatelli G, Laub O, Levi R (2012) Fingerprint-Imprinted Polymer: Rational Selection of Peptide Epitope Templates for the Determination of Proteins by Molecularly Imprinted Polymers. Analytical Chemistry 84 (9):4036-4041. doi:10.1021/ac203422r

10. Yang Y-Q, He X-W, Wang Y-Z, Li W-Y, Zhang Y-K (2014) Epitope imprinted polymer coating CdTe quantum dots for specific recognition and direct fluorescent quantification of the target protein bovine serum albumin. Biosensors and Bioelectronics 54:266-272. doi:http://dx.doi.org/10.1016/j.bios.2013.11.004

11. Wang Y-Z, Li D-Y, He X-W, Li W-Y, Zhang Y-K (2015) Epitope imprinted polymer nanoparticles containing fluorescent quantum dots for specific recognition of human serum albumin. Microchim Acta 182 (7-8):1465-1472. doi:10.1007/s00604-015-1464-1

12. Zhao X-L, Li D-Y, He X-W, Li W-Y, Zhang Y-K (2014) An epitope imprinting method on the surface of magnetic nanoparticles for specific recognition of bovine serum album. Journal

of Materials Chemistry B 2 (43):7575-7582. doi:10.1039/C4TB01381F

13. Yang K, Li S, Liu J, Liu L, Zhang L, Zhang Y (2016) Multiepitope Templates Imprinted Particles for the Simultaneous Capture of Various Target Proteins. Analytical Chemistry 88 (11):5621-5625. doi:10.1021/acs.analchem.6b01247

14. Piletsky SA, Turner APF (2002) Electrochemical Sensors Based on Molecularly Imprinted Polymers. Electroanalysis 14 (5):317-323. doi:10.1002/1521-4109(200203)14:5<317::aid-elan317>3.0.co;2-5

15. Blanco-López MC, Lobo-Castañón MJ, Miranda-Ordieres AJ, Tuñón-Blanco P (2004) Electrochemical sensors based on molecularly imprinted polymers. TrAC, Trends Anal Chem 23 (1):36-48

16. McCluskey A, Holdsworth CI, Bowyer MC (2007) Molecularly imprinted polymers (MIPs): sensing, an explosive new opportunity? Org Biomol Chem 5 (20):3233-3244

17. Prasada Rao T, Kala R (2008) Potentiometric transducer based biomimetic sensors for priority envirotoxic markers--An overview. Talanta 76 (3):485-496

18. Suryanarayanan V, Wu C-T, Ho K-C (2010) Molecularly Imprinted Electrochemical Sensors. Electroanalysis 22 (16):1795-1811. doi:10.1002/elan.200900616

19. Salmi Z, Benmehdi H, Lamouri A, Decorse P, Jouini M, Yagci Y, Chehimi MM (2013) Preparation of MIP grafts for quercetin by tandem aryl diazonium surface chemistry and

photopolymerization. Microchim Acta 180 (15):1411-1419. doi:10.1007/s00604-013-0993-8

20. Bates F, del Valle M (2015) Voltammetric sensor for theophylline using sol–gel immobilized molecularly imprinted polymer particles. Microchim Acta 182 (5):933-942. doi:10.1007/s00604-014-1413-4

21. Huang C-Y, O'Hare D, Chao IJ, Wei H-W, Liang Y-F, Liu B-D, Lee M-H, Lin H-Y (2015) Integrated potentiostat for electrochemical sensing of urinary 3-hydroxyanthranilic acid with molecularly imprinted poly(ethylene-co-vinyl alcohol). Biosensors and Bioelectronics 67:208-213. doi:http://dx.doi.org/10.1016/j.bios.2014.08.018

22. Li S, Liu C, Yin G, Luo J, Zhang Z, Xie Y (2016) Supramolecular imprinted electrochemical sensor for the neonicotinoid insecticide imidacloprid based on double amplification by Pt-In catalytic nanoparticles and a Bromophenol blue doped molecularly imprinted film. Microchim Acta 183 (12):3101-3109. doi:10.1007/s00604-016-1962-9

23. Huang C-Y, Tsai T-C, Thomas JL, Lee M-H, Liu B-D, Lin H-Y (2009) Urinalysis with molecularly imprinted poly(ethylene-co-vinyl alcohol) potentiostat sensors. Biosensors and Bioelectronics 24 (8):2611-2617. doi:http://dx.doi.org/10.1016/j.bios.2009.01.016

24. Lee M-H, Thomas JL, Chang Y-C, Tsai Y-S, Liu B-D, Lin H-Y (2016) Electrochemical sensing of nuclear matrix protein 22 in urine with molecularly imprinted poly(ethylene-co-vinyl alcohol) coated zinc oxide nanorod arrays for clinical studies of

bladder cancer diagnosis. Biosensors and Bioelectronics 79:789-795. doi:http://dx.doi.org/10.1016/j.bios.2016.01.005

25. Navakul K, Warakulwit C, Yenchitsomanus P-t, Panya A, Lieberzeit PA, Sangma C A novel method for dengue virus detection and antibody screening using a graphene-polymer based electrochemical biosensor. Nanomedicine: Nanotechnology, Biology and Medicine. doi:http://dx.doi.org/10.1016/j.nano.2016.08.009

26. Lee M-H, Thomas JL, Chen W-J, Li M-H, Shih C-P, Lin H-Y (2015) Fabrication of Bacteria-imprinted Polymer Coated Electrodes for Microbial Fuel Cells. ACS Sustainable Chemistry & Engineering 3 (6):1190-1196. doi:10.1021/acssuschemeng.5b00138

27. Chen W-J, Lee M-H, Thomas JL, Lu P-H, Li M-H, Lin H-Y (2013) Microcontact Imprinting of Algae on Poly(ethylene-co-vinyl alcohol) for Biofuel Cells. ACS Applied Materials & Interfaces 5 (21):11123-11128. doi:10.1021/am403313p

28. Birnbaumer GM, Lieberzeit PA, Richter L, Schirhagl R, Milnera M, Dickert FL, Bailey A, Ertl P (2009) Detection of viruses with molecularly imprinted polymers integrated on a microfluidic biochip using contact-less dielectric microsensors. Lab on a Chip 9 (24):3549-3556. doi:10.1039/B914738A

29. Lee M-H, O'Hare D, Chen Y-L, Chang Y-C, Yang C-H, Liu B-D, Lin H-Y (2014) Molecularly imprinted electrochemical sensing of urinary melatonin in a microfluidic system.

Biomicrofluidics 8 (5):054115. doi:10.1063/1.4898152

30. Cheng L-P, Young T-H, You W-M (1998) Formation of crystalline EVAL membranes by controlled mass transfer process in water–DMSO–EVAL copolymer systems. Journal of Membrane Science 145 (1):77-90. doi:http://dx.doi.org/10.1016/S0376-7388(98)00063-5

31. Bertrand JA, Pignol D, Bernard JP, Verdier JM, Dagorn JC, Fontecilla-Camps JC (1996) Crystal structure of human lithostathine, the pancreatic inhibitor of stone formation. The EMBO Journal 15 (11):2678-2684

32. Radon TP, Massat NJ, Jones R, Alrawashdeh W, Dumartin L, Ennis D, Duffy SW, Kocher HM, Pereira SP, Guarner L, Murta-Nascimento C, Real FX, Malats N, Neoptolemos J, Costello E, Greenhalf W, Lemoine NR, Crnogorac-Jurcevic T (2015) Identification of a Three-Biomarker Panel in Urine for Early Detection of Pancreatic Adenocarcinoma. Clinical Cancer Research 21 (15):3512-3521. doi:10.1158/1078-0432.ccr-14-2467

33. Lavignac N, Brain KR, Allender CJ (2006) Concentration dependent atrazine–atrazine complex formation promotes selectivity in atrazine imprinted polymers. Biosensors and Bioelectronics 22 (1):138-144. doi:http://dx.doi.org/10.1016/j.bios.2006.03.017

34. El-Sharif HF, Hawkins DM, Stevenson D, Reddy SM (2014) Determination of protein binding affinities within hydrogel-based molecularly imprinted polymers (HydroMIPs). Physical Chemistry Chemical Physics 16 (29):15483-15489. doi:10.1039/C4CP01798F

35. Lakshmi D, Bossi A, Whitcombe MJ, Chianella I, Fowler SA, Subrahmanyam S, Piletska EV, Piletsky SA (2009) Electrochemical Sensor for Catechol and Dopamine Based on a Catalytic Molecularly Imprinted Polymer-Conducting Polymer Hybrid Recognition Element. Analytical Chemistry 81 (9):3576-3584. doi:10.1021/ac802536p

36. Lee M-H, Thomas JL, Li M-H, Shih C-P, Jan J-S, Lin H-Y (2015) Recognition of Rhodobacter sphaeroides by microcontact-imprinted poly(ethylene-co-vinyl alcohol). Colloids and Surfaces B: Biointerfaces 135:394-399. doi:http://dx.doi.org/10.1016/j.colsurfb.2015.07.074

37. Lin H-Y, Ho M-S, Lee M-H (2009) Instant formation of molecularly imprinted poly(ethylene-co-vinyl alcohol)/quantum dot composite nanoparticles and their use in one-pot urinalysis. Biosensors and Bioelectronics 25 (3):579-586. doi:http://dx.doi.org/10.1016/j.bios.2009.03.039

**Legends**

**Figure 1.** The comparison of peptide 2 in Regenerating Islet-Derived 1 Beta (REG1B) protein with non-homologous peptides from REG1A, REG3G, REG3A, REG4 and Aggrecan.

**Figure 2.** (a) Cyclic voltammetry of peptide 4 solutions measured using peptide 4-imprinted coated electrodes using a potentiostat. The calibration curve of (b) peptide 2, (c) peptide 4 and (c) peptide 6 to peptide- and non-imprinted polymer based sensors. The working potential was 300mV (vs. ref. electrode).

**Figure 3.** (a) The effect of the interferents (e.g. albumin, urea and creatinine) at 1.0 ng/mL on peak current response using peptide 4-imprinted coated electrodes. (b) The comparison of the peptide 4 MIP sensors titrated with peptide 4 or REG1B. The working potential was 300mV (vs. ref. electrode).

**Figure 4.** The completive recognition of the imprinted template co-exists with interferents (e.g. albumin, urea and creatinine) at 1.0 $ng \cdot mL^{-1}$. The relative current densities were compared with the original electrochemical response.

**Tables:**

**Table 1.** The peptides of Regenerating Protein 1 Beta (REG1B) used to imprint onto poly(ethylene- *co*-vinyl alcohol)s. Peptides 2, 4 and 6 contain 16, 18 and 13 amino acids and 2, 3 and 3 aromatic or hydrophobic amino acids. The last column indicates the screen of EVALs with highest imprinting effectiveness.

| **Protein** | **Amino acid sequence** | Peptides | Amino acids | | EVAL (mole%) |
|---|---|---|---|---|---|
| | | | Total | Aromatic & Hydrophobic | |
| **REG1B** | MAQTNSFFMLISSLMFLSLSQGQESQTELPNPRISCP EGT NAYRSYCYYFNEDPETWVDADLYCQNMNSG NLVSVLTQAEGAFVASLIKESSTDDSNVWIGLHDPKK | Peptide 6 | 13 | 3 | 27 |
| | NRRWHWSSGSLVSYKSWDTGSPSSANAGYCASL | Peptide 4 | 18 | 3 | 32 |
| | TSCSGFKKWKDESCEKKFSFVCKFKN | Peptide 2 | 16 | 2 | 27 |

## Figures

| 120 | 121 | 122 | 123 | 124 | 125 | 126 | 127 | 128 | 129 | 130 | 131 | 132 | 133 | 134 | 135 | | | (Secreted protein/crystal structure sequence) |
|---|---|---|---|---|---|---|---|---|---|---|---|---|---|---|---|---|---|---|
| 142 | 143 | 144 | 145 | 146 | 147 | 148 | 149 | 150 | 151 | 152 | 153 | 154 | 155 | 156 | 157 | | | |
| S | S | T | G | F | Q | K | W | ***K*** | ***D*** | V | P | C | ***E*** | ***D*** | ***K*** | | | REG1A |
| | C | S | | | **K** | | | | | **E** | **S** | | | **K** | | | | REG1B |
| R | | | | | L | | | | | Y | N | | D | A | | | | REG3G |
| R | | | A | | L | R | | | | Y | N | | N | V | R | | | REG3A |
| | N | N | N | | L | T | | S | S | N | E | | N | K | R | | | REG4 |
| H | E | K | | | | E | | N | | | | | N | Y | H | | | Aggrecan |

Lin et al.- Figure 1

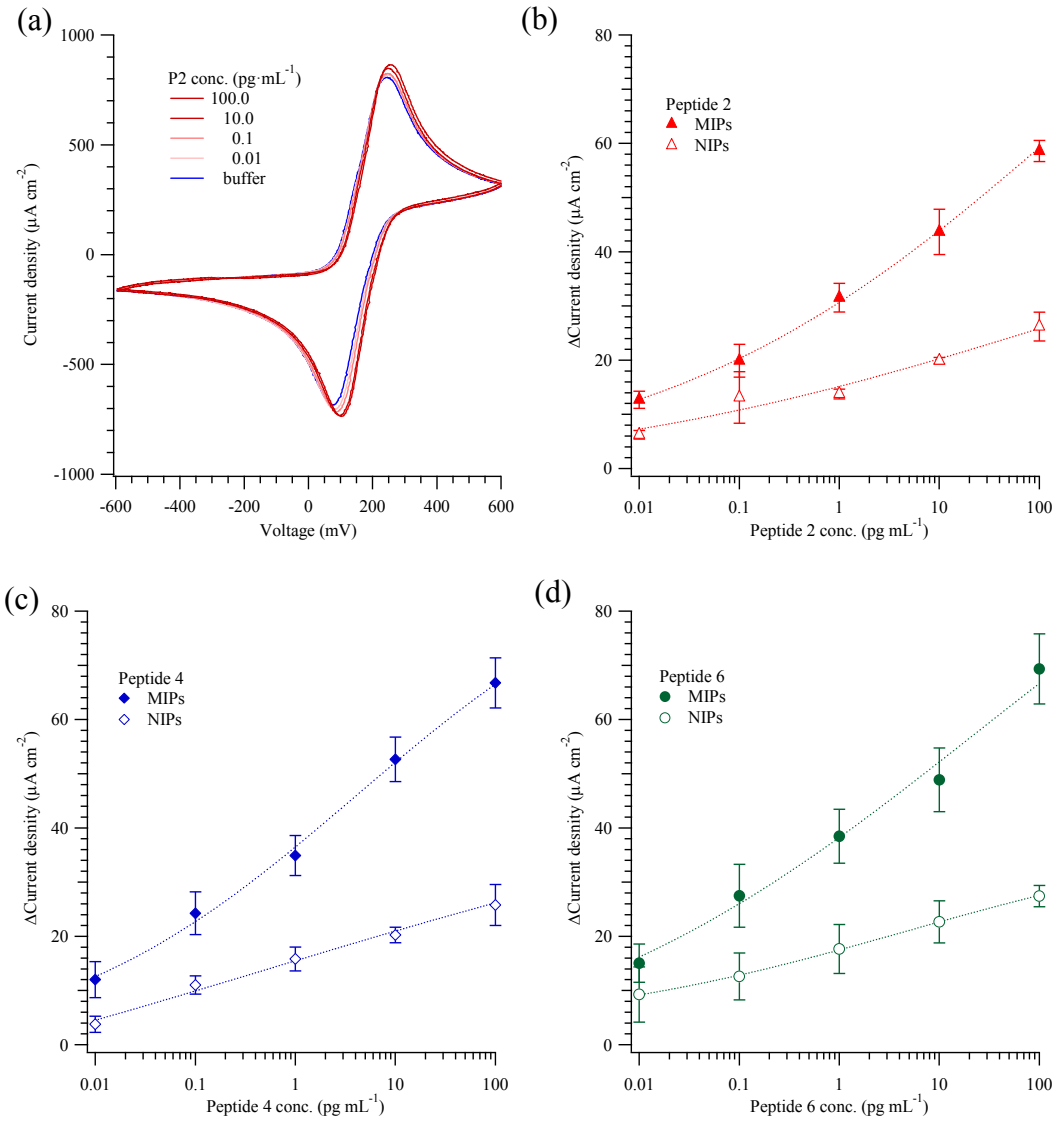


Lin et al.- Figure 2

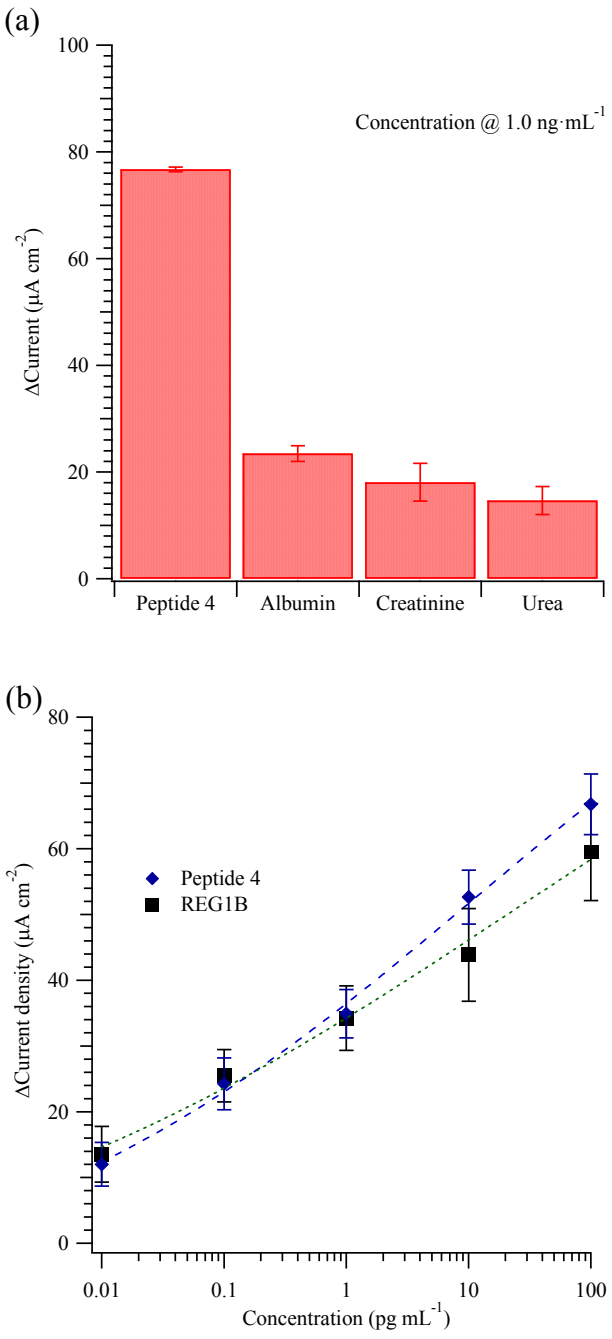


Lin et al.- Figure 3

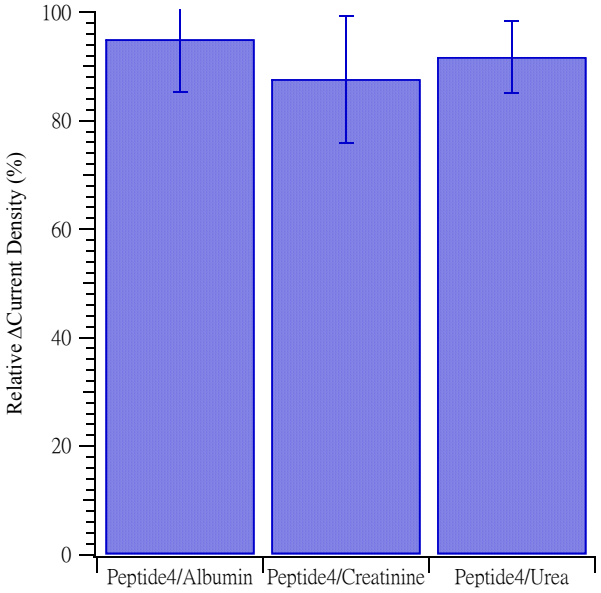


Lin et al.- Figure 4

**Electronic Supporting Material (ESM):**

The possible 2nd choice is peptide 4 (Fig. S1(a)), close to C-terminus part of the protein, 18 amino acids long. Important non-homologous amino acids between REG1A and REG1B: positions 125, 126 GI (neutral/hydrophobic) to DT (negative charge/polar), position 128 A (hydrophobic) to S (polar), position 134 P (aromatic) to A (hydrophobic). The peptide has 1-2 charged amino acids (K/KD). The peptide solubility should be adequate due to 1-2 charged amino acids and seven polar (SSSNYCS) amino acids. Also, there are two bulky, aromatic amino acids (WY) within the sequence. The difference between REG1A and REG1B compared to REG3, REG4 and Aggrecan is substantial, thus cross-reaction is unlikely. Proline 134/112 is at the center of the extended loop, and indeed most of this peptide is within this loop. Positions 135/113 and 136/114 (G and Y) have been proposed to form a $Ca^{+2}$ -binding site (site 1), while positions 128/106 and 130/108 (A and S) are thought to form a second $Ca^{+2}$ -binding site (site 2).

The third candidate peptide, peptide 6 (Fig. S1(b)), is from the middle part of the protein, and is 13 amino acids long. There are modest differences in non-homologous amino-acids between REG1A and REG1B: position 92 G (glycine, neutral) to S (serine, polar), position 96 F (phenylalanine, large hydrophobic) to S (polar). The peptide has four charged amino acids (KEDD). The peptide solubility should be very good due to the four charged amino acids and three polar (STN) amino acids. The difference between REG1A and REG1B compared to REG3, REG4 and Aggrecan is substantial, thus cross-reaction is very unlikely. A large part of this peptide forms an extended loop (positions 90-97), whereas several amino acids (positions 97-99) form the short beta-strand. Furthermore, negative charge amino acids in positions 94/72 and 95/73 (DD) have been proposed to form a contiguous parallel stretch on the protein surface. Notably, position 90/68 (E) is proposed to contribute to the opposite, less acidic surface of the protein.

(a)

| 100 | 101 | 102 | 103 | 104 | 105 | 106 | 107 | 108 | 109 | 110 | 111 | 112 | 113 | 114 | 115 | 116 | 117 | (Secreted protein/crystal structure sequence) |
|---|---|---|---|---|---|---|---|---|---|---|---|---|---|---|---|---|---|---|
| 122 | 123 | 124 | 125 | 126 | 127 | 128 | 129 | 130 | 131 | 132 | 133 | 134 | 135 | 136 | 137 | 138 | 139 | |
| K | S | W | G | I | G | A | P | S | S | V | N | ***P*** | G | Y | C | V | S | REG1A |
| | | | **D** | **T** | | **S** | | | | A | | **A** | | | | A | | REG1B |
| F | A | | E | K | N | P | S | T | I | L | | | | H | | G | | REG3G |
| F | A | | E | R | N | P | S | T | I | S | S | | | H | | A | | REG3A |
| R | | | | | S | G | K | | M | G | G | N | K | H | | R | E | REG4 |
| E | N | | R | P | N | Q | | D | A | A | G | E | D | C | V | | M | Aggrecan |

(b)

| 67 | 68 | 69 | 70 | 71 | 72 | 73 | 74 | 75 | 76 | 77 | 78 | 79 | | | | | | (Secreted protein/crystal structure sequence) |
|---|---|---|---|---|---|---|---|---|---|---|---|---|---|---|---|---|---|---|
| 89 | 90 | 91 | 92 | 93 | 94 | 95 | 96 | 97 | 98 | 99 | 100 | 101 | | | | | | |
| K | ***E*** | S | G | T | ***D*** | ***D*** | F | N | V | W | I | G | | | | | | REG1A |
| | | | **S** | | | | **S** | | | | | | | | | | | REG1B |
| R | S | I | S | N | S | Y | S | Y | I | | | | | | | | | REG3G |
| | S | I | | N | S | Y | S | Y | | | | | | | | | | REG3A |
| | | | | Y | Q | R | S | Q | | | | | | | | | | REG4 |
| | N | N | N | A | Q | | Y | Q | | | | | | | | | | Aggrecan |

**Figure S1.** The comparison of (a) peptide 4 and (b) peptide 6 in Regenerating Islet-Derived 1 Beta (REG1B) protein with non-homologous peptides from REG1A, REG3G, REG3A, REG4 and Aggrecan.

**Table S1.** The current measurement of urine samples by peptide 4-imprinted EVAL coated electrodes. Three urine samples from healthy and pancreatic ductal adenocarcinoma (PDAC) were diluted a thousand and ten thousand times, respectively, and then measured with electrochemical analysis and ELISA (N.D.: not detectable).

| Regimentation | Sample Name | ΔCurrent density ($\mu A \cdot cm^{-2}$) | Converted concentration ($ng \cdot mL^{-1}$) | Mean concentration ($ng \cdot mL^{-1}$) | ELISA results ($ng \cdot mL^{-1}$) |
|---|---|---|---|---|---|
| PDAC 1/10000 | PDAC1 | 59.26 | 206.36 | 205.48±20.96 | 207.05±79.50 |
| | | 59.69 | 225.98 | | |
| | | 58.73 | 184.10 | | |
| | PDAC2 | 57.15 | 131.69 | 137.92±6.62 | 159.51±52.26 |
| | | 57.34 | 137.21 | | |
| | | 57.60 | 144.87 | | |
| | PDAC3 | 53.91 | 66.69 | 62.25±7.01 | 92.30±28.69 |
| | | 53.86 | 65.90 | | |
| | | 52.92 | 54.17 | | |
| HEALTHY 1/1000 | H1 | 34.44 | 0.59 | 0.47±0.12 | N.D. |
| | | 33.06 | 0.46 | | |
| | | 31.74 | 0.36 | | |
| | H2 | 33.09 | 0.46 | 0.55±0.12 | N.D. |
| | | 33.52 | 0.50 | | |
| | | 35.21 | 0.68 | | |
| | H3 | 33.68 | 0.51 | 0.54±0.11 | N.D. |
| | | 32.94 | 0.45 | | |
| | | 35.07 | 0.67 | | |

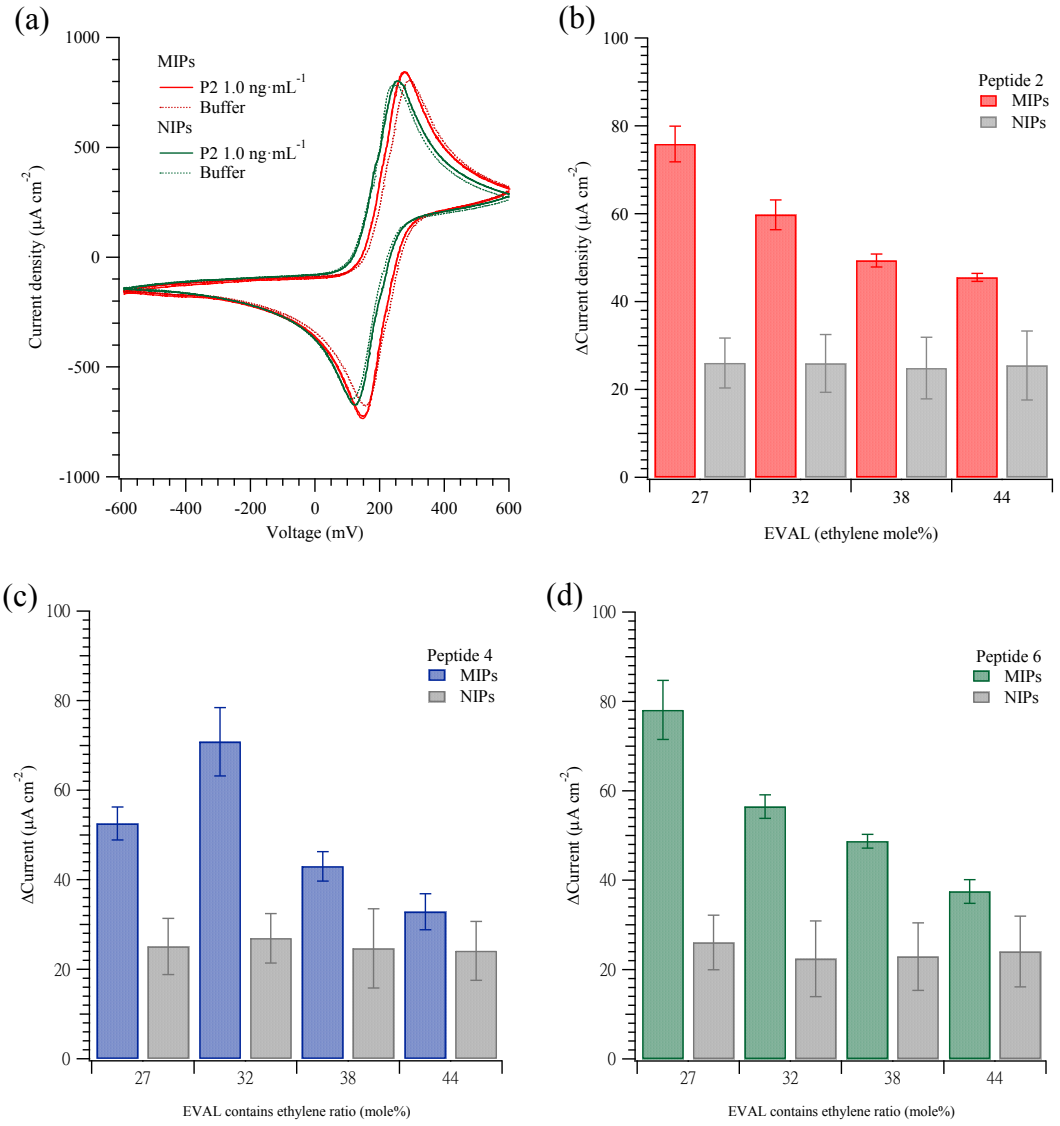


**Figure S2.** (a) Cyclic voltammetry of peptide 2 solutions measured using peptide 2-imprinted and non-imprinted polymer coated electrodes using a potentiostat. Current density difference for the (b) peptide 2-imprinted; (c) peptide 4-imprinted; and (d) peptide 6-imprinted and non-imprinted polymers coated electrode for 1.0 ng·mL$^{-1}$ and buffer solution of target molecules when voltages of 0.36 were applied. The imprinting effectiveness was defined as the ratio of the current density difference of peptides on the MIPs to that on the NIPs of the same composition.

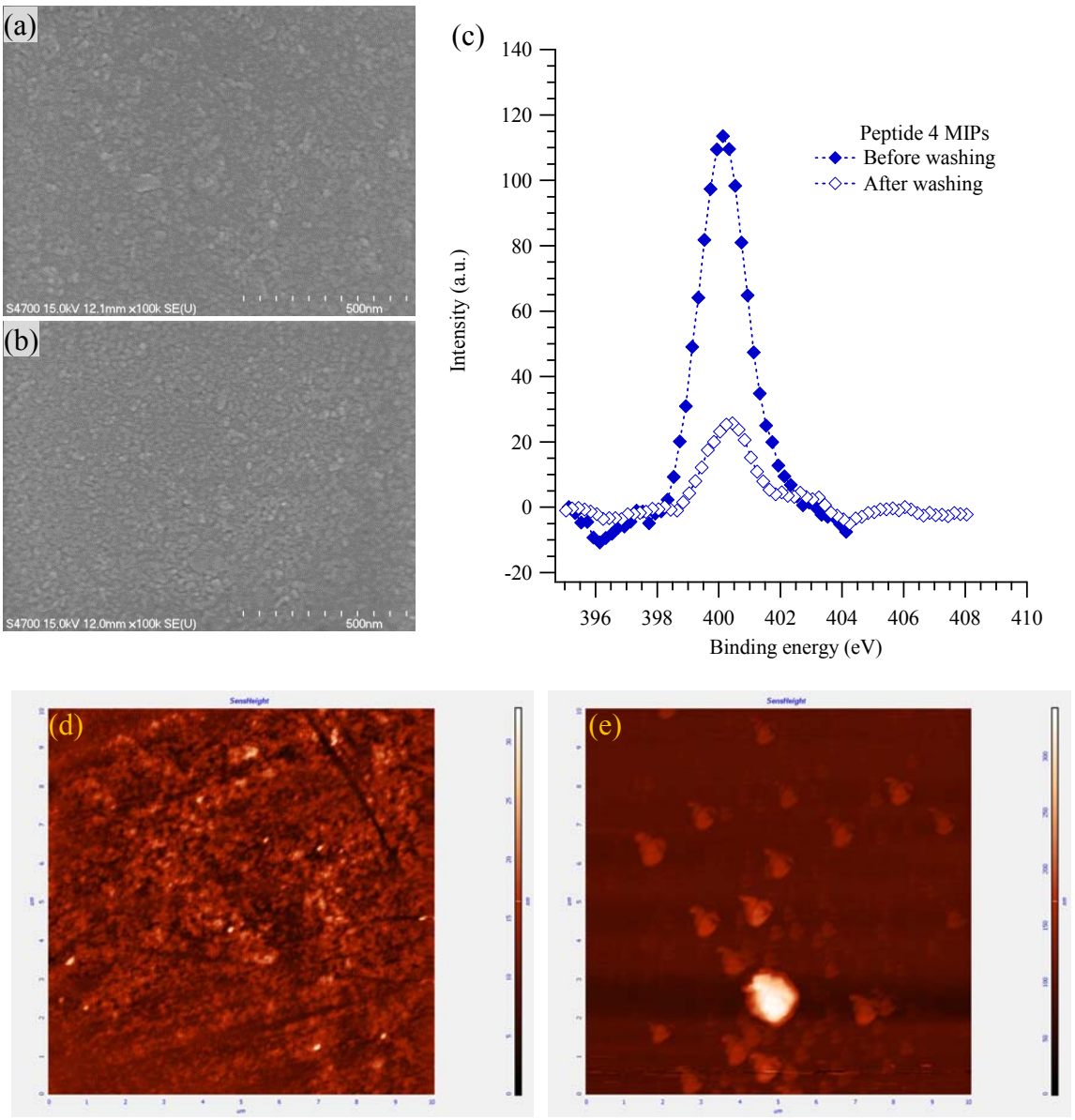


**Figure S3.** The surface morphology of peptide 4-imprinted polymers prepared using 32 mole% of ethylene EVAL (a) before and (b) after template removal of peptide 4. (c) Nitrogen atomic analysis of above surface by electron spectroscopy for chemical analysis (ESCA). AFM images of peptide 4-imprinted polymers prepared using 32 mole% of ethylene EVAL (d) after template removal and (e) after rebinding of peptide 4. The image size is 10x10 $\mu m^2$ and the maximum heights are 34 and 340 nm, respectively.

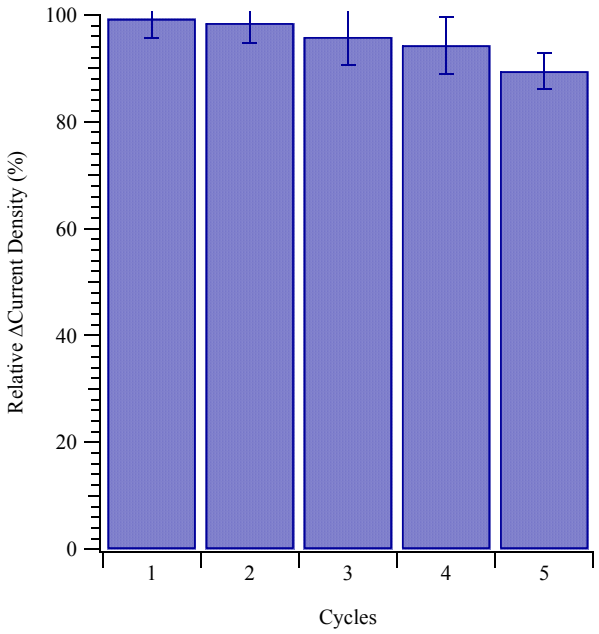


**Figure S4.** The reusability of the peptide 4-imprinted MIP electrode. The electrode was used to measure a 1.0 ng·mL$^{-1}$ solution of peptide 4, rinsed, and then reused for at least 5 cycles.